An L-type calcium-channel gene mutated in incomplete X-linked congenital stationary night blindness

Tim M. Strom[1], Gerald Nyakatura[2], Eckart Apfelstedt-Sylla[3], Heide Hellebrand[1], Birgit Lorenz[4], Bernhard H.F. Weber[5], Krisztina Wutz[1], Nadja Gutwillinger[1], Klaus Rüther[3], Bernd Drescher[2], Christian Sauer[5], Eberhart Zrenner[3], Thomas Meitinger[1], Andre Rosenthal[2] & Alfons Meindl[1]

The locus for the incomplete form of X-linked congenital stationary night blindness (CSNB2) maps to a 1.1-Mb region in Xp11.23 between markers *DXS722* and *DXS255*. We identified a retina-specific calcium channel α_1-subunit gene (*CACNA1F*) in this region, consisting of 48 exons encoding 1966 amino acids and showing high homology to L-type calcium channel α_1–subunits. Mutation analysis in 13 families with CSNB2 revealed nine different mutations in 10 families, including three nonsense and one frameshift mutation. These data indicate that aberrations in a voltage-gated calcium channel, presumably causing a decrease in neurotransmitter release from photoreceptor presynaptic terminals, are a frequent cause of CSNB2.

Congenital stationary night blindness (CSNB, OMIM 310500) is a clinically and genetically heterogeneous non-progressive eye disorder with life-long impairment of night vision and variably reduced day vision. Patients with the 'Schubert-Bornschein' type of CSNB have an electroretinogram (ERG) with essentially normal a-waves in a mixed cone-rod response and small b-waves resulting in a characteristic 'negative' ERG waveform, suggesting functional rod photoreceptor outer segments with a more proximal molecular defect[1]. Complete Schubert-Bornschein lacks rod b-waves and dark adaptation, whereas the incomplete type has residual rod activity and an abnormal cone ERG (refs 2–4). X-linked CSNB (xlCSNB), always of the Schubert-Bornschein type, frequently also manifests reduced visual acuity, myopia, nystagmus and strabismus. Genetic analyses of xlCSNB revealed heterogeneity with at least two loci[5,6]. Complete xlCSNB segregates with markers from Xp11.4-Xp11.3 (CSNB1), and incomplete xlCSNB segregates with markers from Xp11.23 (CSNB2; ref. 7).

Schubert-Bornschein CSNB is thought to result from decreased effectiveness of synaptic transmission between photoreceptors and second-order neurons in the neuroretina[8]. A tie between retinal disease and voltage-gated ion channels was suggested by frog retina studies indicating that glutamate release from photoreceptor presynaptic terminals, important in the transmission of graded potentials, is mediated by L-type (long-lasting) dihydropyridine (DHP)-sensitive calcium channels[9]. L-type calcium channels consist of four subunits (α_1, $\alpha_2\delta$, β and γ), with the calcium-conducting pore located in the α_1-subunit. Three autosomal L-type channel α_1 genes have been cloned thus far: α_{1s} from skeletal muscle[10], α_{1c} from cardiac muscle and brain[11] and α_{1d} from neural and endocrine tissues[12].

We analysed 1000 kb of genomic DNA encompassed by markers *DXS6950* distally and *DXS1331* proximally (http://genome.imb-jena.de). Screening of nonredundant EST database and exon-prediction programs revealed a novel L-type calcium channel α_1-subunit gene spanning 28 kb. Its 3′ and 5′ ends lay 5 kb proximal to the synaptophysin gene and 600 bp distal to a HSP27 pseudogene, respectively (Fig. 1). The 3′ end was represented on two retinal cDNA clones (IMAGE 363620 and AA317815) and was also identified during the characterization of sequences around the synaptophysin locus[13]. RT-PCR with primers from non-conserved exon regions was performed using retinal cDNA as a template, as the 3′ end is represented in two retinal cDNA clones. Sequencing of overlapping PCR products identified 48 exons, a coding sequence of 5901 nucleotides and a predicted protein 1966 amino acids in length (219.5 kD). Except for splice acceptor sites for introns 2, 19 and 33, all intron splice acceptor and donor sequences followed the GT-AG rule. Forty-four of forty-eight exons were predicted by GENSCAN (ref. 14), 43 by GRAIL (ref. 15) and 36 by GENEFINDER.

5′-RACE and RT-PCR extended the transcript sequence 62 bp upstream of the first ATG. A possible TATA box was found 103 bp upstream of the first ATG (TSSG program). Analysis of sequences around the first ATG suggested that *CACNA1F* lacks a Kozak consensus sequence. CpG islands were present within the *HSP27* pseudogene, located 1000 bp upstream of the first exon (68.2% G+C, 0.79 observed/expected, 628 bp), around exon 4 (62.7% G+C, 1.18 CpG observed/expected, 311 bp) and in intron 6 (56.3% G+C, 1.09 CpG observed/expected, 158 bp). At the 3′ end, RACE product sequences and the sequence of IMAGE clone 363620 identified a 3′ UTR of only 73 nucleotides with a polyadenylation signal (AATAAA) 25 bp downstream of the stop codon.

Database analysis showed a 55–62% overall amino-acid sequence identity between CACNA1F and L-type calcium channel α_1-subunits (Fig. 2*a*,*b*). The amino-acid identity to P- and N-type calcium channels was approximately 35%. Sequence iden-

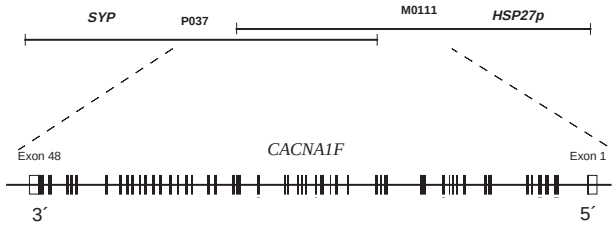

Fig. 1 Physical mapping of *CACNA1F*. The gene was identified on cosmids LLNLc110P037 and LLNLc110M0111 (ref. 22) by direct sequencing with subsequent use of exon-prediction programs. It is flanked by synaptophysin *(SYP)* and a HSP pseudogene *(HSP27p)*.

[1]*Abteilung Medizinische Genetik der Ludwig-Maximilians-Universität, Goethestr. 29, 80336 München, Germany.* [2]*Institut für Molekulare Biotechnologie, Am Beutenberg 11, 07745 Jena, Germany.* [3]*Augenklinik der Universität, 72076 Tübingen, Germany.* [4]*Ophthalmogenetik der Augenklinik der Universität, 93042 Regensburg, Germany.* [5]*Institut für Humangenetik, Am Hubland, 97074 Würzburg, Germany. Correspondence should be addressed to A.M. e-mail: alfons@pedgen.med.uni-muenchen.de*

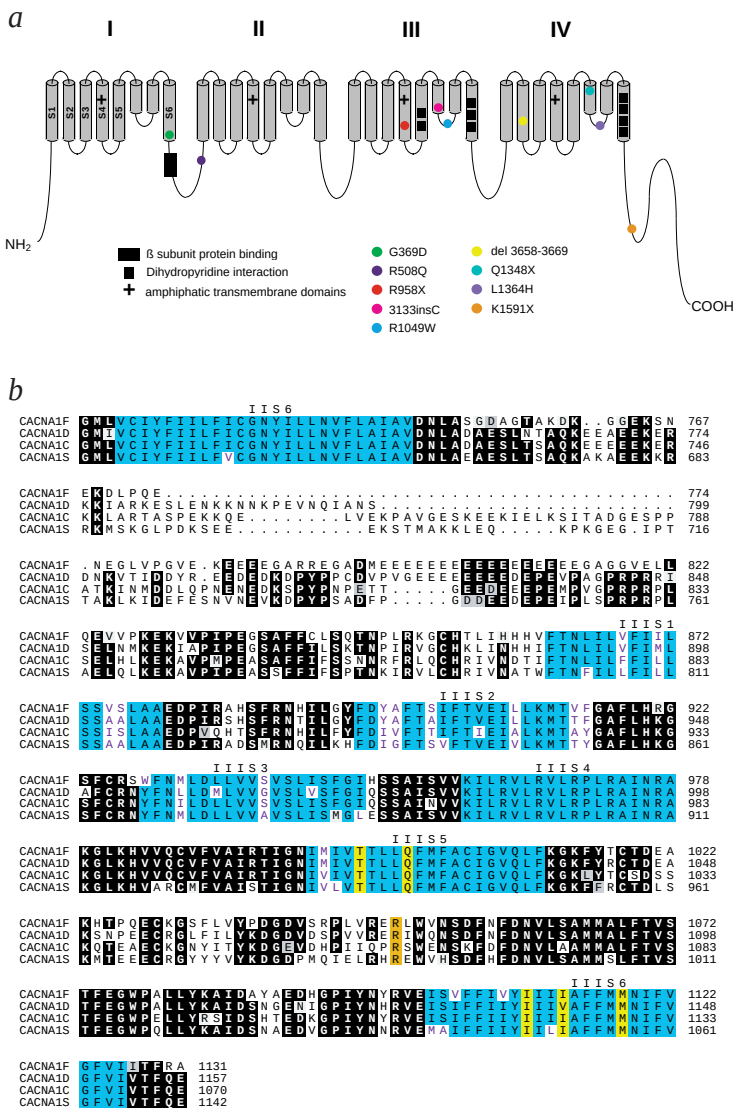

Fig. 2 *CACNA1F* encodes the α_1-subunit of an L-type calcium channel. **a**, Diagram of the voltage-gated calcium channel α_1-subunits. Each α_1-subunit contains four repeat domains, which closely resemble a single K^+-channel α-subunit in structure and basic function. Each repeat domain contains six transmembrane domains (S1–S6). The amphipathic transmembrane domain is indicated by a plus sign. The segment to which the β-subunit protein binds is indicated by a black box, the positions of the amino acids conferring DHP binding are indicated by a black square. The mutations are depicted by coloured circles. ***b***, Partial alignment of CACNA1F with other human L-type calcium channels: CACNA1D (PIR:JH0564), CACNA1C (GenBank:L29529), CACN1AS (PIR:A55645). The figure shows the alignment from transmembrane domain IIS6 to IIIS6. The putative transmembrane domains are blue, the amino acids conferring dihydropyridine binding yellow, and the missense mutation R1049W orange.

tity between CACNA1F and the L-type channels was highest in the putative membrane-spanning regions and the intracellular loop linking repeat domains III and IV. The charged residues of the S4 regions, important as voltage sensors[16], were also conserved. The amino acids at the DHP binding sites at IIIS5/S6 and IVS6 (refs 17,18) and the β-unit binding sequence after the first repeat domain[19] were well conserved. These data support CACNA1F as a new member of the L-type calcium channel α_1-subunit family.

Zoo-blot hybridization containing *Eco*RI-digested genomic DNA with a 3′ probe (jm8-13) produced a single band per species, indicating no cross hybridization (Fig. 3*a*). In human genomic DNA, a 5.8-kb band corresponded with the expected *Eco*RI restriction fragment. Hybridization of this probe to northern blots revealed a 6.3-kb signal in retina only under stringent washing conditions (Fig. 3*b*). Faint signals were observed in skeletal muscle, kidney and pancreas under low washing stringency (data not shown). Previously reported skeletal muscle expression[13] may result from use of a less specific probe. Tissue specificity was further confirmed by RT-PCR using *CACNA1F*-specific primers, which produced fragments from retinal, but not heart or brain, cDNA (data not shown). RNA *in situ* hybridization of the jm8-13 antisense probe on paraffin-embedded mouse eye sections revealed transcriptional activity in the retinal outer-nuclear (ONL) and inner-nuclear (INL) cell layers. A weaker hybridization signal was observed in the ganglion-cell layers (GCL; Fig. 4). The ONL contains photoreceptor cell bodies, whereas the INL consists of horizontal, bipolar and amacrine cells. Ganglion cells are the final retinal output neurons. Hybridization of the sense probe demonstrated no detectable signal (data not shown).

We then investigated 13 xlCSNB index patients presenting with either reduced visual acuity, nystagmus, strabismus or a combination of these findings. There was a consistent incomplete phenotype within each family. X-linked inheritance was determined by pedigree analysis, resulting in a pattern of affected males in

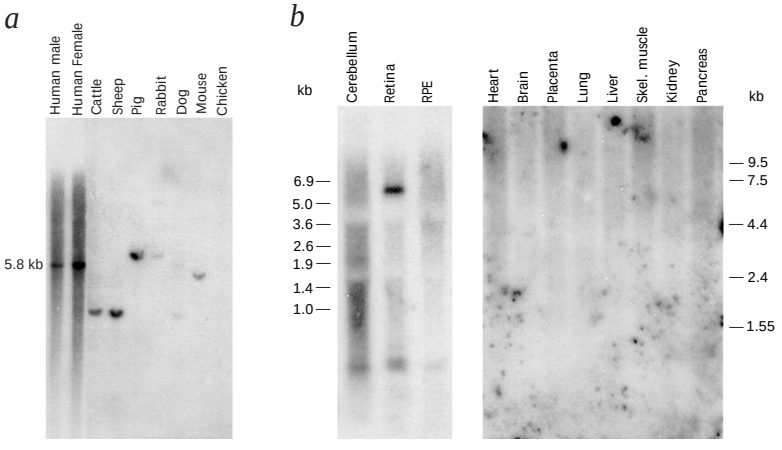

Fig. 3 Retinal specificity of *CACNA1F*. ***a***, Zoo-blot hybridization with probe jm8-13 (586 bp) revealed only a single band per species. Washing was under stringent conditions; lanes with human DNA were exposed 1 d, lanes with non-human DNA were exposed 5 d. ***b***, Northern-blot analysis with probe jm8-13 revealed specific retinal expression. A 6.3-kb transcript was observed under stringent conditions in retinal tissue only. Cerebellum, retina and retinal pigment epithelium (RPE) lanes contain total RNA (left), the other tissues are represented by polyA$^+$-RNA. Exposure was for 10 d.

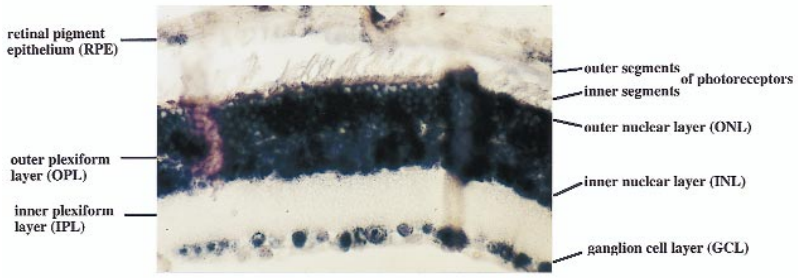

Fig. 4 RNA *in situ* hybridization. The jm-13 antisense probe was used to hybridize mouse eye sections. Specific signals can be seen in the ONL and INL with a weak hybridization in the GCL. No signal can be seen in RPE or inner plexiform layer (IPL).

two or more generations with intervening asymptomatic females, except families xlCSNB13 and 14, where the affected males were brothers or maternal first cousins (families 1, 2; ref. 4).

Mutation screening in index patients was performed using single-stranded conformation polymorphism (SSCP; Fig. 5*a*). Thirty-nine of forty-eight exons were screened with primer pairs based on exon-intron boundaries, and exons with an abnormal migration pattern were directly sequenced (Fig. 5*b*, Table 1). In ten of the thirteen families, nine different mutations were identified in affected males and their carrier mothers, and no mutations were seen in unaffected brothers tested. The five missense mutations and the 12-bp deletion were not found in 120 control chromosomes by SSCP. Family xlCSNB06 had two missense mutations; the second affected a non-conserved leucine (L849P). The missense mutation in family xlCSNB02 segregated in the family with a lod score of 2.1 (data not shown). The four mutations causing truncated and deleted proteins strongly implicated *CACNA1F* loss-of-function mutations as the cause of CSNB2. The significance of the missense mutations (Table 1) was supported by high structural conservation of the affected amino acids between α_1-subunits.

It is thought that Schubert-Bornschein CSNB results from defective neurotransmission between photoreceptors and bipolar cells *via* a decrease either in the amount of transmitter released or the effectiveness of the transmitter at the postreceptoral site[8]. *Xenopus laevis* 'reduced-retina' investigations show that glutamate neurotransmitter release from photoreceptor presynaptic terminals is mediated by L-type calcium channels of unknown class[9,20]. Assuming a similar mechanism, ERG results in our patients, together with the protein implied, are more supportive of decreased transmitter release with essentially normal photoreceptor current as shown by the dark- and light-adapted a-waves, but abnormal inner nuclear layer activity as reflected in the rod and cone b-waves. ERG b-waves are mainly generated by Müller glial cells but also depend on the light response of depolarizing ON-bipolar cells[21]. We suggest that mutations in the α_1-subunit of the L-type calcium channel impair the influx of Ca^{2+} required for tonic glutamate release from photoreceptor presynaptic terminals in darkness. The lowered glutamate levels would inadequately stimulate the postreceptor bipolar cell membranes, thus keeping the ON-bipolar cells relatively depolarized (light-adapted) and limiting synaptic gain between first- and second-order retinal neurons. Other mechanisms or retinal sites of action for Schubert-Bornschein CSNB have also to be considered, as indicated by the result of RNA *in situ* hybridization.

We present the first report of mutations in a voltage-gated L-type calcium channel α_1-subunit gene causing an inherited human eye disease. These findings may enable investigations into pharmacologic agents to regulate retinal calcium metabolism and neurotransmitter release. In addition, the mutation data presented provide evidence that complete and incomplete xlCSNB result from non-allelic heterogeneity.

Table 1 • *CACNA1F* mutations in families with xlCSNB

Family	Mutation	Exon	Type
02	1106G→A, G369D	8	missense
03	1523G→A, R508Q	13	missense
06	1523G→A, R508Q	13	missense
14	2172C→T, R958X	24	stop
22	3133insC	27	frameshift
13	3145C→T, R1049W	27	missense
05	del3658-3669	30	12-bp deletion
21	4042C→T, Q1348X	35	stop
15	4091T→A, L1364H	35	missense
10	4771A→T, K1591X	41	stop

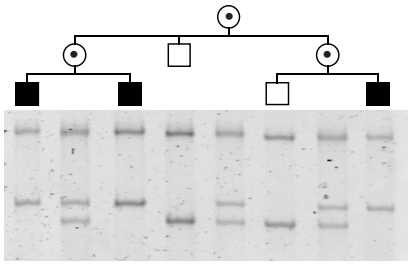

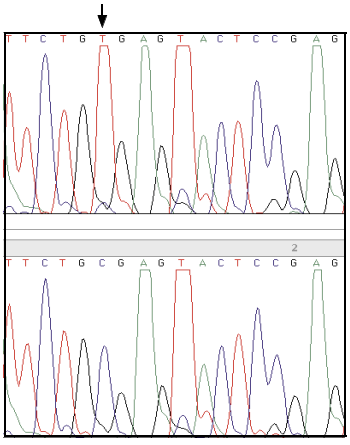

Fig. 5 Mutation analysis in family xlCSNB14. ***a***, Co-segregation of incomplete CSNB with SSCP band shifts. Affected males and female carriers are represented by standard symbols. ***b***, Identification of a C→T transition at nucleotide position 2172 in exon 24 causing a stop codon (R958X).

Methods

Clinical details. The clinical methods have been published in detail elsewhere[2,4]. Every patient had a general ophthalmologic examination. Best-corrected visual acuity at distance ranged from 20/30 to 20/400. All family members had normal peripheral visual fields on Goldman perimetry (except xlCSNB13 and 14, not tested). Dark adaptometry showed elevation of rod dark adaption final thresholds from 0.3 to 2.5 log units. Dark-adapted Ganzfeld ERGs showed attenuated rod b-waves, and a 'negative' ERG waveform to bright flashes, in other words a large a-wave followed by a small b-wave, the peak of which was below the ERG baseline (except in family xlCSNB14). In the light-adapted ERG, there was a decrease in cone amplitude and delay of peak times; 30 Hertz flicker stimuli evoked a characteristic double-peak response in most patients.

Genomic sequencing. Overlapping human cosmid clones from the Xp11.23 region[22] were sequenced using a combination of the shotgun approach and primer walking strategy, as described[23]. Briefly, the cosmids were subcloned in pUC18 plasmids and the shotgun plasmid clones were sequenced from both ends using standard M13 primers and dye terminator chemistry. The data were collected using ABI 377 automatic sequencers (PE Applied Biosystems) and assembled using GAP4 (ref. 24). Remaining gaps were closed using custom-made primers on plasmid

templates, PCR products or cosmid DNA. The genomic sequences are posted (http://genome.imb-jena.de).

Sequence analysis. Homology searches against the nonredundant and EST databases were performed using BLAST and FASTA. *CACNA1F* was predicted using GENSCAN (ref. 14), GRAIL (ref.15) and GENEFINDER (C. Wilson, L. Hillier and P. Green, pers. comm.) as exon prediction programs. Genome-wide repeats were identified using the REPEATMASKER program. Sequence alignments were performed using the Global Alignment Program (GAP) and CLUSTALW for multiple alignments.

RT-PCR and RACE. RT-PCR was performed using retinal cDNA (1–2 ng; Clontech) as a template. RACE was performed with the Marathon cDNA Amplification Kit (Clontech). The primers designed in non-conserved regions of the predicted cDNA sequence are available on request. The specific probe jm8-13 was obtained with the following primer pairs: jm8-13F, 5´–GTGTCTCTGCCTGTCGG–3´; jm8-13R, 5´–TGCGCAGTGGGCCACTG–3´.

Northern-blot analysis. The northern blot with cerebellum, retina and RPE contained 12 µg total RNA. The multiple-tissue northern blot (MTN1) contained polyA$^+$-RNA from heart, brain, placenta, lung, liver, skeletal muscle, kidney and pancreas (2 µg each; Clontech). Hybridization with probe jm8-13 was performed in Church buffer at 65 °C; washing was done with 0.01×SSC at either 30 °C (non-stringent) or 60 °C (stringent).

In situ hybridization on paraffin sections. The 586-bp fragment jm-13 was used as a probe for *in situ* hybridization. The PCR fragment was cloned into pBluescript II SK(+) (Stratagene) and linearized using *Xho*I or *Not*I restriction enzymes. Transcription reactions were carried out according to the manufacturer's instructions using either T7 or T3 RNA polymerase in the presence of 11-digoxygenin UTP (Boehringer). Eyecups of adult CD1 mice (Charles River Laboratories) were fixed in 4% paraformaldehyde in PBS at 4 °C overnight, washed in PBS, dehydrated in a graded isopropanol series, infiltrated with chloroform and embedded in paraffin. Sections (5 mm) were mounted on polylysine-coated slides, dried overnight at 42 °C and stored at 4 °C. RNA *in situ* hybridizations were performed as described[25], except sections were hybridized at 65 °C with digoxygenin-labelled probes (1 mg/ml).

SSCP mutation analysis. Genomic DNA was isolated from peripheral EDTA-blood by standard techniques. *CACNA1F* exons were amplified with intronic primers (obtainable on request). Amplified fragments from 39 exons (available on request) were analysed by SSCP using Hydrolink gels (AT Biochem.) at 20 °C with and without glycerol[26]. Staining was performed with ^{TM}VistraGreen and detection performed with a FluorImager (Molecular Dynamics). Variant bands were reamplified and used for direct sequencing with both the sense and antisense primer using cycle sequencing on Applied Biosystems 377 PRISM automated sequencers.

Accession numbers. *CACNAIF* cDNA, AJ224874; *CACNAIF* genomic sequence, AJ002616 (submitted to EMBL).

Acknowledgements

We are grateful to the families who participated in this study. We thank B. Wissinger and M. Andrassi for sending DNA samples, K.B. Jedele for extensive help in manuscript preparation and H. Achatz for technical assistance. The work was supported by the German Federal Ministry for Education, Research and Technology by a grant to A.R. and A.M. as well as by Deutsche Retinitis Pigmentosa Gesellschaft by a grant to N.G.

Received 25 March; accepted 26 May, 1998.

1. Schubert, G. & Bornschein, H. Beitrag zur Analyse des menschlichen Electroretinogramms. *Ophthalmologica* **123**, 396–413 (1952).
2. Ruether, K., Apfelstedt-Sylla, E. & Zrenner, E. Clinical findings in patients with congenital stationary night blindness of the Schubert-Bornschein type. *Ger. J. Ophthalmol*. **2**, 429–435 (1993).
3. Miyake, Y., Horiuchi, M., Ota, I. & Shiroyama, N. Characteristic ERG flicker anomaly in incomplete congenital stationary night blindness. *Invest. Ophthalmol. Vis. Sci*. **28**, 1816–1823 (1987).
4. Lorenz, B., Andrassi, M. & Miliczek, K.D. Die inkomplette kongenitale stationäre Nachtblindheit (CSNB). Eine wichtige Differentialdiagnose des kongenitalen Nystagmus. *Klin. Monatsbl. Augenheilkd*. **208**, 48–55 (1996).
5. Bergen, A.A.B., ten Brink, J.B., Riemslag, F., Schuurman, E.J.M. & Tijmes N. Localization of a novel X-linked congenital stationary night blindness locus: Close linkage to the RP3 type retinitis pigmentosa gene region. *Hum. Mol. Genet*. **4**, 931–935 (1995).
6. Bech-Hansen, N.T. & Pearce, W.G. Manifestations of X-linked congenital stationary night blindness in three daughters of an affected male: Demonstration of homozygosity. *Am. J. Hum. Genet*. **52**, 71–77 (1993).
7. Boycott, K.M. *et al*. Evidence for genetic heterogeneity in X-linked congenital stationary night blindness. *Am. J. Hum. Genet*. **62**, 865–875 (1998).
8. Hood, D.C. & Greenstein, V. Models of the normal and abnormal rod system. *Vision Res*. **30**, 51–68 (1990).
9. Schmitz, Y. & Witkovsky, P. Dependence of photoreceptor glutamate release on a dihydropyridine-sensitive calcium channel. *Neuroscience* **78**, 1209–1216 (1997).
10. Hogan, K., Powers, P.A. & Gregg R.G. Cloning of the human skeletal muscle a subunit of the dihydropyridine-sensitive L-type calcium channel (CACNL1A3). *Genomics* **24**, 608–609 (1994).
11. Schultz, D. *et al.* Cloning, chromosomal localization, and functional expression of the α_1 subunit of the L-type voltage-dependent calcium channel from normal heart. *Proc. Natl Acad. Sci. USA* **90**, 6228–6232 (1990).
12. Williams, M.E. *et al.* Structure and functional expression of alpha 1, alpha 2, and beta subunits of a novel human neuronal calcium channel subtype. *Neuron* **8**, 71–84 (1992).
13. Fisher, S.E. *et al.* Sequence-based exon prediction around the synaptophysin locus reveals a gene-rich area containing novel genes in human proximal Xp. *Genomics* **46**, 340–347 (1997).
14. Burge, C. & Karlin, S. Prediction of complete gene structures in human genomic DNA. *J. Mol. Biol.* **268**, 78–94 (1997).
15. Uberbacher, E.C. & Mural, R.J. Locating protein-coding regions in human DNA-sequences by a multiple sensor neural network approach. *Proc. Natl Acad. Sci. USA* **88**, 11261–11265 (1992).
16. Stuhmer, W. *et al.* Structural parts involved in activation and inactivation of the sodium channel. *Nature* **339**, 597–603 (1989).
17. Schuster, A. *et al.* The IVS6 segment of the L-type calcium channel is critical for the action of dihydropyridines and phenylalkylamines. *EMBO J.* **15**, 2365–2370 (1996).
18. Sinnegger, M.J. *et al.* Nine L-type amino acid residues confer full 1,4-dihydropyridine sensitivity to the neuronal calcium channel alpha1A subunit. Role of L- type Met1188. *J. Biol. Chem*. **272**, 27686–27693 (1997).
19. Pragnell, M. *et al.* Calcium channel β-subunit binds to a conserved motif in the I-II cytoplasmic linker of the a_1-subunit. *Nature* **368**, 67–71 (1994).
20. Witkovsky, P., Schmitz, Y., Akopian, A., Krizaj, D. & Tranchina, D. Gain of rod to horizontal cell synaptic transfer: relation to glutamate release and a dihydropyridine-sensitive calcium current. *J. Neurosci*. **17**, 7297–7306 (1997).
21. Stockton, M. & Slaughter, M.M. B-wave of the electroretinogram. A reflection of ON-bipolar cell activity. *J. Gen. Physiol*. **93**, 101–122 (1989).
22. Schindelhauer, D. *et al.* Long range map of a 3.5-Mb region in Xp11.23 with a sequence ready map from a 1.1 Mb gene-rich interval. *Genome Res.* **6**, 1056–1069 (1996).
23. Craxton, M. Cosmid sequencing. *Methods Mol. Biol.* **23**, 149–167 (1993).
24. Bonfield, J.K., Smith, K.F. & Staden, R. A new DNA sequence assembly program. *Nucleic Acids Res.* **24**, 4992–4999 (1995).
25. Leimeister, C., Bach, A. & Gessler, M. Developmental expression patterns of mouse sFRP genes encoding members of the secreted frizzled related protein family. *Mech. Dev.* (in press).
26. Meindl, A. *et al.* A gene (RPGR) with homology to the RCC1 guanine nucleotide exchange factor is mutated in X-linked retinitis pigmentosa (RP3). *Nature Genet.* **13**, 35–42 (1996).